Original Article

Effect of 15-Deoxy-$\Delta^{12,14}$-prostaglandin J_2 Nanocapsules on Inflammation and Bone Regeneration in a Rat Bone Defect Model

Qi Tang, Li-Li Chen, Fen Wei, Wei-Lian Sun, Li-Hong Lei, Pei-Hui Ding, Jing-Yi Tan, Xiao-Tao Chen, Yan-Min Wu

Department of Oral Medicine, The Second Affiliated Hospital of School of Medicine of Zhejiang University, Hangzhou, Zhejiang 310009, China

Abstract

Background: 15-Deoxy-$\Delta^{12,14}$-prostaglandin J_2 (15d-PGJ_2), one of the major metabolites from prostaglandin D2 in arachidonic acid metabolic pathway, has potential anti-inflammatory properties. The objective of this study was to explore the effects of 15d-PGJ_2-loaded poly(D,L-lactide-co-glycolide) nanocapsules (15d-PGJ_2-NC) on inflammatory responses and bone regeneration in local bone defect.

Methods: The study was conducted on 96 Wistar rats from June 2014 to March 2016. Saline, unloaded nanoparticles, free 15d-PGJ_2 or 15d-PGJ_2-NC, were delivered through a collagen vehicle inside surgically created transcortical defects in rat femurs. Interleukin-6 (IL-6), interleukin-1 beta (IL-1β), and tumor necrosis factor-alpha (TNF-α) levels in the surrounding soft tissue were analyzed by Western blot and in the defect by quantitative real-time polymerase chain reaction over 14 days. Simultaneously, bone morphogenetic protein-6 (BMP-6) and platelet-derived growth factor-B (PDGF-B) messenger RNA (mRNA) in the defect were examined. New bone formation and EphrinB2 and osteoprotegerin (OPG) protein expression in the cortical defect were observed by Masson's Trichrome staining and immunohistochemistry over 28 days. Data were analyzed by one-way analysis of variance. Least-significant difference and Dunnett's T3 methods were used with a bilateral $P < 0.05$.

Results: Application of l5d-PGJ_2-NC (100 μg/ml) in the local bone defect significantly decreased IL-6, IL-1β, and TNF-α mRNA and protein, compared with saline-treated controls ($P < 0.05$). l5d-PGJ_2-NC upregulated BMP-6 and PDGF-B mRNA ($P < 0.05$). New bone formation was observed in the cortical defect in l5d-PGJ_2-NC-treated animals from 7th day onward ($P < 0.001$). Expression of EphrinB2 and OPG presented early on day 3 and persisted through day 28 in 15d-PGJ_2-NC group ($P < 0.05$).

Conclusion: Stable l5d-PGJ_2-NC complexes were prepared that could attenuate IL-6, IL-1β, and TNF-α expression, while increasing new bone formation and growth factors related to bone regeneration.

Key words: 15-Deoxy-$\Delta^{12,14}$-prostaglandin J_2; Interleukin-1 Beta; Interleukin-6; Nanocapsules; Osteogenesis

Introduction

Periodontal disease is an infectious disease resulting in inflammation within the supporting tissues of the teeth, progressive attachment loss, and bone loss, which is recognized to be initiated by host's innate and adaptive immune responses to a vast array of multiple biofilm-associated microorganisms, particularly Gram-negative bacteria.[1,2]

Moreover, inflammatory cytokines, such as interleukin-6 (IL-6), interleukin-1 beta (IL-1β), and tumor necrosis factor-alpha (TNF-α), could be detected in the periodontal lesions, and their overproduction seems to be tightly associated with tissue destruction.[3,4] Thus, dampening of IL-6, IL-1β, and TNF-α expression would probably become a plausible therapeutic approach for periodontal diseases.

Previous studies demonstrated that during experimental periodontitis, a balance existed between beneficial immune regulation and impaired host defense, which suggested that the use of effective anti-inflammatory agents which

Access this article online

Quick Response Code:

Website: www.cmj.org

DOI: 10.4103/0366-6999.198924

Address for correspondence: Dr. Yan-Min Wu, Department of Oral Medicine, The Second Affiliated Hospital of School of Medicine of Zhejiang University, Hangzhou, Zhejiang 310009, China
E-Mail: wym731128@126.com

Received: 28-09-2016 **Edited by:** Peng Lyu

How to cite this article: Tang Q, Chen LL, Wei F, Sun WL, Lei LH, Ding PH, Tan JY, Chen XT, Wu YM. Effect of 15-Deoxy-$\Delta^{12,14}$-prostaglandin J_2 Nanocapsules on Inflammation and Bone Regeneration in a Rat Bone Defect Model. Chin Med J 2017;130:347-56.

contributed to modulation of the host response might reduce the severity of inflammation, periodontal connective tissue degradation, and bone loss.[5,6] The cyclopentenone-type prostaglandin (PG), 15-Deoxy-$\Delta^{12,14}$-prostaglandin J_2 (15d-PGJ_2), possessed a wide spectrum of physiological activities.[7,8] Gilroy *et al*.[9,10] observed a late peak in the production of 15d-PGJ_2 with an exacerbating effect of a nonsteroidal anti-inflammatory drug during the late stages of the inflammatory response. Subsequently, 15d-PGJ_2 was reported to suppress IL-6 in osteoblast-like MC3T3E-1 cells[11] and produce potential anti-inflammatory effects in various experimental models.[7,9,12] In addition, 15d-PGJ_2 was found to be involved in the regulation of bone metabolism.[12,13] Napimoga *et al*.[13] reported that a low dose of 15d-PGJ_2 administered systemically could induce osteoblast activity, significantly favoring the production of osteonectin and Type I collagen through osteoblast cells, decrease the receptor activator for nuclear factor-κB ligand (RANKL), and increase osteoprotegerin (OPG) expression.

As reported by earlier studies,[7,9-12] 15d-PGJ_2 exhibited anti-inflammatory properties and might play an important role in the modulation of bone metabolism. However, due to low aqueous solubility, only a relatively low amount of 15d-PGJ_2 administered in a biological system was found to be available to produce physiological effects.[7] Further improvement of the *in vivo* efficiency of 15d-PGJ_2 using formulation strategies such as nano-carrier systems, especially biodegradable nanoparticles, might be feasible for therapeutic applications. Current data indicated that 15d-PGJ_2 could be well incorporated into poly (D,L-lactide-co-glycolide, PLGA) nanocapsules, as an efficient carrier system, with improved biocompatibility, low immunogenicity, and little toxicity. Most importantly, 15d-PGJ_2-loaded PLGA nanocapsule (15d-PGJ_2-NC) suspension was significantly more effective than pure 15d-PGJ_2 due to the gradual release of the compound.[12,14,15] The 15d-PGJ_2-NC (10 μg/kg) was also demonstrated to have anti-inflammatory activity and to decrease the expression levels of pro-inflammatory cytokines in Carrageenan-induced peritonitis, while the same dose of 15d-PGJ_2 did not achieve the same effect. Furthermore, 15d-PGJ_2 was detectable in the serum even 24 h after its administration.[15]

In the present study, levels of IL-6, IL-1β, and TNF-α were tested to evaluate the anti-inflammatory activity of 15d-PGJ_2-NC. IL-6 could be produced by many different cells, such as monocytes, fibroblasts, endothelial cells, macrophages, lymphocytes (T-cells and B-cells), and keratinocytes.[16] In the bone microenvironment, IL-6, a multifunctional cytokine produced by osteoblasts, played a major role in the mediation of inflammatory and immune responses to injury.[17] IL-1β and TNF-α could promote IL-6 synthesis by osteoblasts.[18] All these cytokines were observed to stimulate osteoclast proliferation, differentiation, and accelerate bone resorption by a variety of biological mechanisms.[11]

To verify the effect of 15d-PGJ_2-NC on osteogenetic activities, several factors related to bone regeneration and bone repair, which required a complex orchestration of regulatory stimuli including secretion of growth factors, were examined. Bone morphogenetic proteins (BMPs) belonged to the transforming growth factor-beta (TGF-β) superfamily, which was thought to be involved at different stages of osteoblast differentiation.[19] BMP-6, in particular, had drawn attention due to its unique role in the early differentiation of osteoprogenitor cells and initiation of bone regeneration.[20-23] A study conducted by Chiu *et al*.[24] showed that application of BMP-6 onto surgically created supra-alveolar defects enhanced periodontal wound healing/regeneration. In addition to BMPs, platelet-derived growth factor (PDGF) was shown to enhance new bone formation by modulating recruitment and proliferation of osteoprogenitor cells, and increasing synthesis of collagen, alkaline phosphatase, and osteocalcin.[20,22,24] Zhang *et al*.[25] reported that the release of PDGF-B could recruit and differentiate mesenchymal cells, allowing significantly new bone formation in critical-sized defects in ovariectomized rat femurs. EphrinB2, a membrane protein, was mostly expressed on the surface of osteoclasts, as well as on osteoblasts. The EphrinB2/EphB4 pathway might maintain bone homeostasis through regulating the differentiation of both osteoblasts and osteoclasts. Zhao *et al*.[26] demonstrated the mutual cross-activation of EphrinB2 and EphB4 present on the surface of the osteoblasts. Stimulation of EphB4 by EphrinB2 was considered a positive signal transduction event, which promoted osteoblast differentiation and maturation. Simultaneously, the activation of EphrinB2 and the generation of negative signals might inhibit osteoclast differentiation. Thus, the upregulated EphrinB2 expression increased the differentiation of osteoblasts and decreased that of osteoclasts.[26] OPG, a member of the TNF superfamily, expressed on osteoblasts and bone marrow stromal cells, was known as an osteoclast inhibitor during bone metabolism. OPG could competitively bind to RANKL and prevent the over-binding of RANKL and its receptor, the receptor activator of nuclear factor-kB, leading to bone resorption.[27,28] Currently, considerable efforts were made to identify drugs capable of inhibiting RANKL or increasing OPG to adjust the RANKL/OPG ratio, which would potently inhibit bone resorption in the treatment of several diseases. Thus, the aims of this study were to prepare 15d-PGJ_2-NC with stable characteristics and evaluate its effect on several inflammatory cytokines, such as IL-1β, IL-6, and TNF-α, as well as on bone regeneration by the amount of new bone formation and expression of growth factors in the rat critical femur bone defect model.

Methods

Surgical procedures

Ninety-six male Wistar rats, weighing 300–350 g, were randomly divided into different groups. The experimental protocol was conducted in compliance with the regulations

of the Second Affiliated Hospital of School of Medicine of Zhejiang University from June 2014 to March 2016. Two rats were housed in each cage with free access to normal laboratory diet and water. After 7 days of acclimation, the animals were anesthetized by intramuscular injection of sodium pentobarbital at a dosage of 75 mg/kg body weight. The surgical area was shaved and then disinfected with 75% ethyl alcohol. A 3-cm incision was made through skin and muscles on the dorsal side parallel to the long axis of both the left and right femoral bones. The periosteum was carefully removed to expose the surface of the bone. Subsequently, a 5 mm × 1.5 mm transcortical defect was prepared through the cortical bone into the bone marrow in the mid-shaft area using dental steel burs at low speed with abundant sterile saline irrigation. Resorbable collagen sponges were used to deliver the drug. The collagen sponge was soaked with 30 μl of sterile saline (S group), unloaded nanoparticles (K group), free 15d-PGJ_2 (F group), or 15d-PGJ_2-NC (N group) solution (See "Supplementary information" for detailed preparation and characterization of 15d-PGJ_2-loaded PLGA nanocapsule suspension), and gently packed inside the defect of each animal (N = 96, n = 3). The muscles were repositioned and closed using bioresorbable suturing material. Finally, the skin was closed using stainless steel wound clips. The animals were monitored daily after surgery.

Western blotting

On days 1, 3, 7, and 14, the adjacent soft tissues were collected and prepared by homogenization and lysis at 4°C. After centrifugation at 13,000 ×g for 15 min at 4°C, the total protein concentration was tested using the BCA assay. Protein extracts (40 μg per sample) were separated in a 12% sodium dodecyl sulfate-polyacrylamide gels and transferred onto polyvinylidene difluoride membranes. After incubation with the primary antibodies against IL-6 (1:1000, Abcam, USA), IL-1β (1:1000, Abcam, USA), TNF-α (1:1000, CST, USA), and glyceraldehyde-3-phosphate dehydrogenase (GAPDH) (1:5000, CST, USA), the membranes were incubated for 1 h at room temperature with a rabbit monoclonal secondary antibody (1:5000). Signals were detected with the ECL detection system. Densitometry analysis was performed using the ImageJ 2X software (Rawak Software Inc., the Tomancak Laboratory, Dresden, Germany) to scan immunoreactive bands.

Quantitative real-time polymerase chain reaction

On days 1, 3, 7, and 14 after surgery, muscle tissues around the cortical defect and the bone defect areas were obtained to evaluate the messenger RNA (mRNA) expression of IL-6, IL-1β, TNF-α, BMP-6, and PDGF-B. Total RNA was isolated by the TRIZOL method, according to the manufacturer's recommendations (Invitrogen, USA). RNA samples were resuspended in diethylpyrocarbonate-treated water and stored at −80°C. The RNA concentration was determined from the optical density (OD) reading using a microvolume spectrophotometer. The complementary DNA (cDNA) template for the real-time polymerase chain reaction (RT-PCR) was synthesized from 1 μg of total RNA. The reaction was conducted using the First-Strand cDNA Synthesis Kit, following the manufacturer's recommendations (Toyobo, Japan). The reverse transcription reaction mixture (2 μl) was added to 18 μl of the PCR reaction, including specific PCR primers for IL-6 (5'-CCAATTTCCAATGCTCTCCT-3' and 5'-ACCACAGTGAGGAATGTCCA-3'), IL-1β (5'-ATGAGAGCATCCAGCTTCAAATC-3' and 5'-CACACTAGCAGGTCGTCATCATC-3'), TNF-α (5'-CCAGAACTCCAGGCGGTGTC-3' and 5'-GGCTACGGGCTTGTCACTCG-3'), BMP-6 (5'-GCAGAAGGAGATCTTGTCGG-3' and 5'-GTCTCTGTGCTGATGCTCCT-3'), PDGF-B (5'-CCGCTCCTTTGATGACCTTCA-3' and 5'-CAGCCCGAGCAGCGCTGCACCTC-3'), and GAPDH (5'-CAAGTTCAACGGCACAGTCAAGG-3' and 5'-ACATACTCAGCACCAGCATCACC-3'). The quantitative RT-PCR (qRT-PCR) was performed with FastStart DNA Master Plus SYBR Green (Genecopoeia, USA) with the following conditions: preheating at 95°C for 10 min, followed by 40 cycles of denaturation at 95°C for 15 s, annealing at 60°C for 20 s, and extension at 72°C for 20 s.

Morphometric analysis

On days 3, 7, 14, and 28 after surgery, the animals were sacrificed by a lethal intraperitoneal dose of sodium pentobarbital. Transcardial perfusion was performed with 0.1% heparinized (heparin sodium 1000 U/ml) phosphate buffer (0.1 mol/L, pH = 7.4) for approximately 10 min. Tissues were fixed using 4% paraformaldehyde in phosphate buffer (0.1 mol/L, pH = 7.4) for 20 min. The femoral bone was isolated, removed, and postfixed in the same solution for 48 h. The samples were decalcified using 10% ethylenediaminetetraacetic acid (EDTA), with pH 7.2 at 4°C. The EDTA solution was changed for every 3 days. The tissues were dehydrated and embedded in paraffin wax by routine procedure. The embedded specimens were cut in a plane perpendicular to the long axis of the femoral bone into 5-μm thick sections. Sections were stained with Masson's Trichrome staining and examined under a light microscope. The area inside the connecting lines of the four corners of the cortical defect outline was considered as the total cortical defect area. The bone formation in the cortical defect area was calculated automatically by the Image-Pro Plus 6.0 software (Media Cybernetics, Silver Spring, MD USA).

Immunohistochemistry

Three sections from each defect were immunostained for the detection of OPG and EphrinB2. After deparaffinization, the slides were rehydrated in a series of increasing concentrations of ethanol. To block endogenous peroxidase activity, the sections were incubated in 3% hydrogen peroxide in methanol for 10 min. After being washed three times for 5 min each time in phosphate buffer, sections were incubated in 10% normal Goat serum to inhibit nonspecific binding to OPG and EphrinB2. Overnight incubation was performed

at 4°C with rabbit anti-rat OPG/EphrinB2 antibodies (1:100, Abcam, USA). After extensive washing, biotinylated anti-rabbit Ig was applied as a secondary antibody for 30 min. The sections were washed again before the addition of streptavidin-biotin peroxidase complexes for 30 min. Finally, immunoreactivity was visualized by incubating for 5 min in a solution containing 3,3'-diaminobenzidine (DAB) and 0.02% hydrogen peroxide. Counterstaining with hematoxylin was performed for 1 min. A negative control was processed through the complete immunohistochemistry procedure except for the omission of the primary antibody. Areas of new bone formation and immune-positive staining for the expression of growth factors within the cortical defect area were assessed as described above and presented as a percentage of the total cortical defect area. The positive area of immunostaining was calculated automatically by the Image-Pro Plus 6.0 software. The intensity of the light source of the microscope was calibrated before every session with the same control slide.

Statistical analysis

Data are reported as mean ± standard deviation (SD). A mean value was calculated for each cortical defect of every animal, and data from animals of the same group were pooled to form a group mean. Data were analyzed by one-way analysis of variance (ANOVA) by Statistical Package of Social Sciences for Windows (version 19.0, SPSS Inc., Chicago, IL, USA). Least-significant difference (LSD) method was used for data with equal variance. For data with heterogeneity of variance, Dunnett's T3 method was applied. Statistical significance was set at bilateral $P < 0.05$.

Results

15-Deoxy-$\Delta^{12,14}$-prostaglandin J_2-nanocapsules inhibit interleukin-1β, interleukin-6, and tumor necrosis factor-α protein expression in the peri-defect tissues

All animals recovered rapidly after surgery and remained in good health during the study. Protein levels of IL-6, IL-1β, and TNF-α were shown in Figure 1 and Table 1.

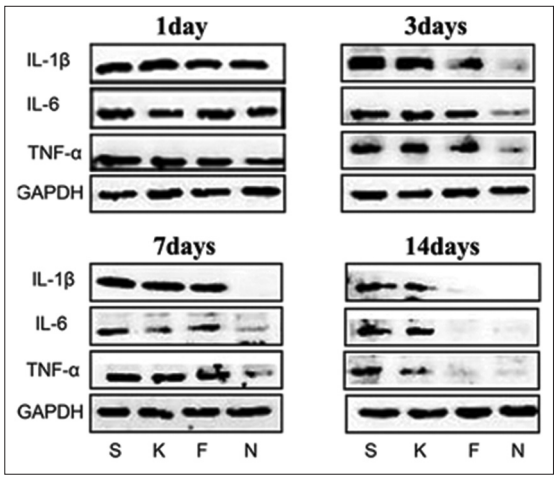

Figure 1: Effects of 15d-PGJ2 on IL-6, IL-1β, and TNF-α protein expression in the peri-defect tissues. A 5 mm × 1.5 mm transcortical defect was prepared through the cortical bone into the bone marrow in the midshaft area in rats. Protein expression levels of IL-6, IL-1β, and TNF-α in groups treated with saline (S), empty nanocapsules (K), free 15d-PGJ2 (F), and 15d-PGJ2-NC (N) were analyzed by Western blotting on days 1, 3, 7, and 14. 15d-PGJ2-NC: 15-Deoxy-Δ12,14-prostaglandin J2 nanocapsules; IL-1β: Interleukin-1 beta; IL-6: Interleukin-6; TNF-α: Tumor necrosis factor-alpha; GAPDH: Glyceraldehyde-3-phosphate dehydrogenase.

Table 1: Densitometry analysis of IL-1β, IL-6, and TNF-α scanned immunoreactive bands in Western blotting

Groups (n = 3)	IL-1β			
	Day 1	Day 3	Day 7	Day 14
S	1.46 ± 0.022	1.66 ± 0.013	1.32 ± 0.009	0.73 ± 0.004
K	1.22 ± 0.014	1.75 ± 0.014	1.33 ± 0.006	0.43 ± 0.006
F	1.08 ± 0.000	0.74 ± 0.024*†	0.96 ± 0.013	0*†
N	0.78 ± 0.004*†	0.09 ± 0.006*†‡	0.05 ± 0.003*†‡	0*†
Groups (n = 3)	**IL-6**			
	Day 1	**Day 3**	**Day 7**	**Day 14**
S	1.47 ± 0.027	0.81 ± 0.007	0.53 ± 0.005	0.66 ± 0.006
K	0.73 ± 0.008*	1.01 ± 0.002	0.20 ± 0.002*	0.59 ± 0.015
F	1.34 ± 0.029	0.64 ± 0.019†	0.42 ± 0.009	0.01 ± 0.000*†
N	0.69 ± 0.014*‡	0.11 ± 0.004*†‡	0.05 ± 0.003*†‡	0 ± 0.004*†
Groups (n = 3)	**TNF-α**			
	Day 1	**Day 3**	**Day 7**	**Day 14**
S	1.46 ± 0.014	0.79 ± 0.008	1.09 ± 0.023	0.57 ± 0.004
K	1.00 ± 0.033	0.99 ± 0.008	0.97 ± 0.030	0.26 ± 0.011*
F	1.09 ± 0.009	0.73 ± 0.008	1.09 ± 0.023	0.03 ± 0.002*†
N	0.57 ± 0.003*†‡	0.12 ± 0.005*†‡	0.15 ± 0.003*†‡	0.02 ± 0.000*†

Values represent the mean ± SD of three animals for each group. *P<0.05 versus groups S; †P<0.05 versus groups K; ‡P<0.05 versus groups F. IL-1β: Interleukin-1 beta; IL-6: Interleukin-6; TNF-α: Tumor necrosis factoralpha; S: Saline; K: Empty nanocapsules; F: Free 15Deoxy△12,14-prostaglandin J2; N: 15-deoxy△12,14-prostaglandin J2 nanocapsules; SD: Standard deviation.

Compared with corresponding levels in the controls (S and K groups), IL-6, IL-1β, and TNF-α were significantly downregulated by 15d-PGJ_2-NC on days 1, 3, 7, and 14 ($P < 0.05$). From days 1 to 14, the immunoreactive bands in the 15d-PGJ_2-NC-treated animals weakened and disappeared gradually. However, the inhibiting effect of 15d-PGJ_2 on these inflammatory cytokines was only shown on days 3 and 14 for IL-1β and IL-6, respectively, and day 14 for TNF-α [Table 1]. Empty PLGA nanocapsules did not show the same anti-inflammatory effect.

15-Deoxy-$\Delta^{12,14}$-prostaglandin J_2-nanocapsules inhibit interleukin-1β, interleukin-6, and tumor necrosis factor-α messenger RNA expression in cortical defect area

qRT-PCR analysis was used to determine the effects of 15d-PGJ_2 and 15d-PGJ_2-NC on the release of inflammatory mediators, such as IL-6, IL-1β, and TNF-α [Table 2]. In the bone marrow, the relative mRNA levels of IL-6, IL-1β, and TNF-α were significantly decreased in animals treated with 15d-PGJ_2-NC, compared with saline-treated and empty nanocapsule controls on days 1 to 14 ($P < 0.05$). However, the influence of 15d-PGJ_2 on the mRNA expression was obvious on days 1 and 14 for IL-1β ($P < 0.05$), days 1, 3, and 7 for IL-6 ($P < 0.05$), and days 1, 3, and 14 for TNF-α ($P < 0.05$), which is weaker than that of 15d-PGJ_2-NC.

15-Deoxy-$\Delta^{12,14}$-prostaglandin J_2 upregulates bone morphogenetic protein-6 and platelet-derived growth factor-B messenger RNA expression in cortical defect area

As observed in Table 3, the levels of BMP-6 and PDGF-B were statistically significantly upregulated in 15d-PGJ_2-NC-treated animals, compared with the controls (S and K groups) ($P < 0.05$). Enhanced expression of BMP-6 was shown on all the 4 time points in groups induced by 15d-PGJ_2, with statistically significant difference on days 3, 7, and 14 ($P < 0.05$). However, elevated mRNA level of PDGF-B was only detected on day 14 in 15d-PGJ_2-treated group. No difference in the level of BMP-6 or PDGF-B between the S and K groups was observed.

15-Deoxy-$\Delta^{12,14}$-prostaglandin J_2 increases new bone formation in cortical defect area

As shown in Figure 2, blood clot and loose connective tissue were present in the cortical defect area on day 3. Either no bone trabeculae or remnants of the collagen sponge were detected. Specimens harvested from day 7 revealed dense connective tissue with some immature new bone trabeculae near the bone marrow cavity. On day 14, increased amounts of trabecular bone were observed in the cortical areas. On day 28, specimens showed increased mature bone formation in all animals. Volumes of the newly formed bone trabeculae are summarized in Figure 2b. 15d-PGJ_2-NC increased the new bone formation on days 7, 14, and 28, while the effect of 15d-PGJ_2's lasted from days 7 to 14 ($P < 0.001$).

15-Deoxy-$\Delta^{12,14}$-prostaglandin J_2-nanocapsules upregulate EphrinB2 and osteoprotegerin protein expression in cortical defect area

As Figure 3 showed, that the EphrinB2 was expressed on both osteoclasts and osteoblasts. Most of the positive

Table 2: Relative mRNA expression of IL-1β, IL-6, and TNF-α in the cortical defect area analyzed by qRT-PCR

Groups ($n = 3$)	IL-1β			
	Day 1	Day 3	Day 7	Day 14
S	1.07 ± 0.29	1.02 ± 0.24	1.04 ± 0.36	1.02 ± 0.23
K	0.85 ± 0.34	0.97 ± 0.35	0.95 ± 0.13	1.17 ± 0.11
F	0.69 ± 0.13*	0.63 ± 0.09	0.83 ± 0.14	0.68 ± 0.13*,†
N	0.41 ± 0.13*,†	0.29 ± 0.18*,†,‡	0.47 ± 0.10*,†	0.17 ± 0.02*,†,‡
Groups ($n = 3$)	**IL-6**			
	Day 1	Day 3	Day 7	Day 14
S	1.00 ± 0.12	1.00 ± 0.134	1.00 ± 0.10	1.01 ± 0.23
K	1.13 ± 0.07	1.02 ± 0.38	1.11 ± 0.25	1.04 ± 0.24
F	0.76 ± 0.03†	0.52 ± 0.13*,†	0.56 ± 0.05*	0.77 ± 0.11
N	0.28 ± 0.09*,†	0.28 ± 0.09*,†	0.36 ± 0.18*,†	0.18 ± 0.06*,†,‡
Groups ($n = 3$)	**TNF-α**			
	Day 1	Day 3	Day 7	Day 14
S	1.05 ± 0.40	1.05 ± 0.39	1.05 ± 0.40	1.01 ± 0.20
K	1.20 ± 0.14	0.87 ± 0.16	0.91 ± 0.07	1.01 ± 0.19
F	0.67 ± 0.04*	0.44 ± 0.06*	1.31 ± 0.24	0.64 ± 0.06*,†
N	0.62 ± 0.10*,†	0.38 ± 0.10*,†	0.74 ± 0.21*,‡	0.31 ± 0.05*,†,‡

Values represent the mean ± SD of three animals for each group. *P<0.05 versus groups S; †P<0.05 versus groups K; ‡P<0.05 versus groups F. IL-1β: Interleukin-1 beta; IL-6: Interleukin-6; TNF-α: Tumor necrosis factor-alpha; qRT-PCR: Quantitative real-time polymerase chain reaction; S: Saline; K: Empty nanocapsules; F: Free 15-Deoxy-$\Delta^{12,14}$-prostaglandin J_2; N: 15-deoxy-$\Delta^{12,14}$-prostaglandin J_2 nanocapsules; SD: Standard deviation; mRNA: Messenger RNA.

Table 3: Relative mRNA expression of PDGF-B and BMP-6 in the cortical defect area analyzed by qRT-PCR

Groups ($n = 3$)	BMP-6				PDGF-B			
	Day 1	Day 3	Day 7	Day 14	Day 1	Day 3	Day 7	Day 14
S	1.20 ± 0.12	1.00 ± 0.13	1.01 ± 0.21	1.01 ± 0.11	1.07 ± 0.49	1.01 ± 0.19	1.01 ± 0.13	1.01 ± 0.14
K	1.36 ± 0.32	1.46 ± 0.53	1.46 ± 0.30	1.76 ± 0.13	0.74 ± 0.25	0.72 ± 0.36	0.92 ± 0.08	1.94 ± 0.51
F	2.05 ± 0.27	4.36 ± 0.14*,†	2.34 ± 0.59*	3.50 ± 0.17*,†	1.08 ± 0.25	1.13 ± 0.20	1.03 ± 0.06	2.39 ± 0.56*
N	5.18 ± 0.68*,†,‡	2.86 ± 0.28*,†	4.82 ± 0.76*,†,‡	5.37 ± 0.84*,†,‡	4.68 ± 0.20*,†,‡	2.94 ± 0.33*,†,‡	2.31 ± 0.31*,†,‡	4.04 ± 0.80*,†

Values represent the mean ± SD of three animals for each group. *P<0.05 versus groups S; †P<0.05 versus groups K; ‡P<0.05 versus groups F. BMP-6: Bone morphogenetic protein-6; PDGF-B: Platelet-derived growth factor-B; qRT-PCR: Quantitative real-time polymerase chain reaction; S: Saline; K: Empty nanocapsules; F: Free 15-Deoxy-$\Delta^{12,14}$-prostaglandin J_2; N: 15-Deoxy-$\Delta^{12,14}$-prostaglandin J_2 nanocapsules; SD: Standard deviation; mRNA: Messenger RNA.

staining cells were osteoblasts. Osteoclast was polynuclear cell and the size was bigger than the osteoblast. The OPG was expressed on osteoclasts, osteoblasts, bone lining cells, and even osteocytes [Figure 4].

Expression of EphrinB2 and OPG presented early on day 3 and persisted through day 14. Maximal expression of these bone growth factors was observed on day 7. 15d-PGJ_2-NC statistically significantly increased the area of cells positively stained for EphrinB2 and OPG ($P < 0.05$). Compared with the S group, greater positive staining of EphrinB2 and OPG was also observed in animals treated with 15d-PGJ_2, with or without a statistically significant difference. The time-dependent expression patterns of EphrinB2 and OPG are summarized in Table 4. No significant difference in both the expression of EphrinB2

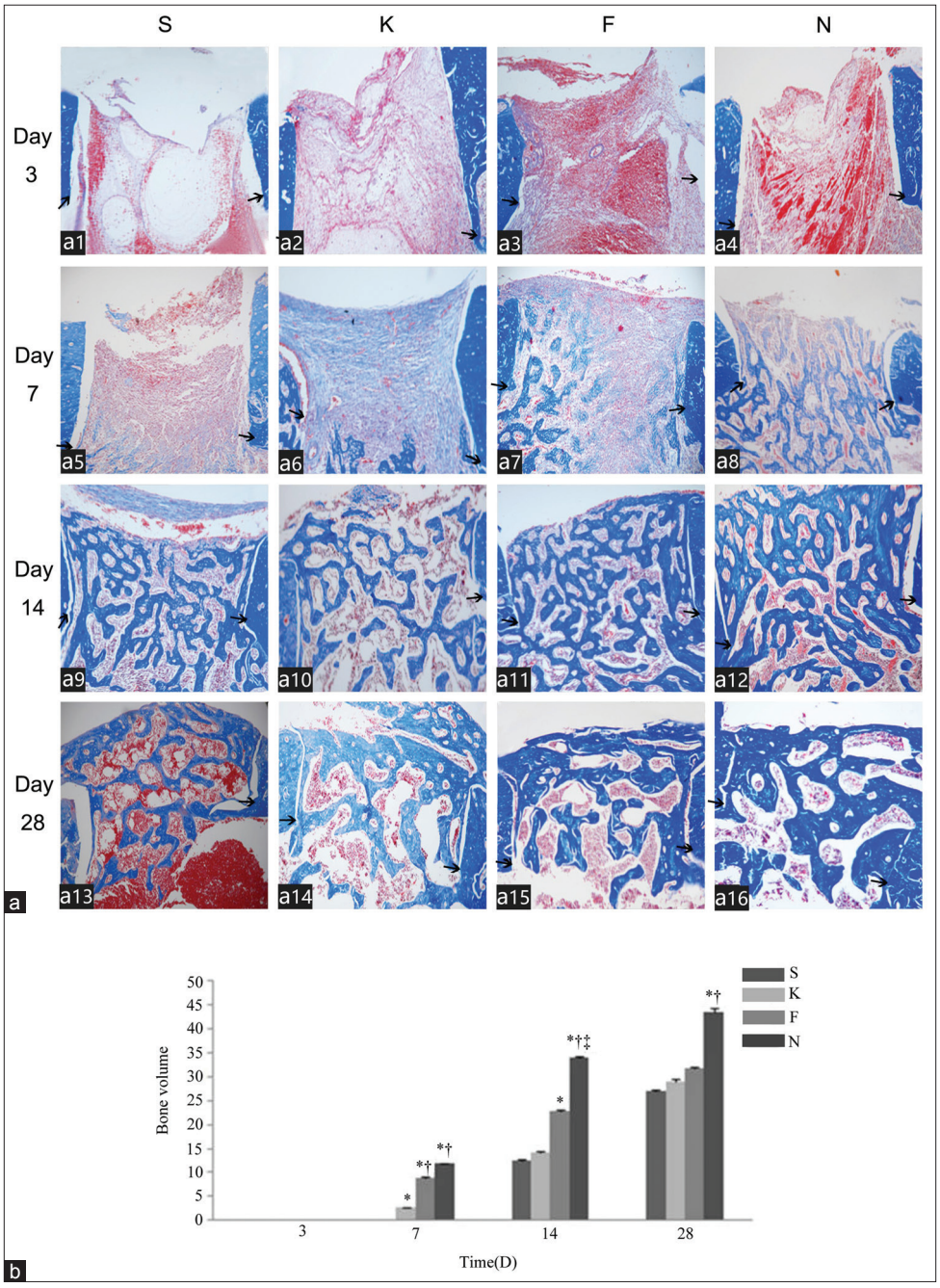

Figure 2: Effect of 15d-PGJ_2 on new bone formation in the cortical defect area. (a) The new bone formation was examined in specimens from animals treated with saline (a1, a5, a11 and a13), empty nanocapsules (a2, a6, a10 and a14), free 15d-PGJ_2 (a3, a7, a11 and a15), and 15d-PGJ_2-NC (a4, a8, a12 and a16) on days 3 (a1-a4), 7 (a5-a8), 14 (a9-a12), and 28 (a13-a16) after surgery, respectively. Black arrows indicated the margin of the surgically created cortical bone wound (Masson's Trichrome, original magnification ×100). (b) Semi-quantitative evaluation of bone formation in the cortical defect area. Three sections from each group were obtained on days 3, 7, 14, and 28. Values represent the mean ± standard deviation of three sections. *$P < 0.05$ versus groups S; †$P < 0.05$ versus groups K; ‡$P < 0.05$ versus groups F. 15d-PGJ_2-NC: 15-Deoxy-$\Delta^{12,14}$-prostaglandin J_2 nanocapsules; S: Saline; K: Empty nanocapsules; F: Free 15-Deoxy-$\Delta^{12,14}$-prostaglandin J_2; N: 15-Deoxy-$\Delta^{12,14}$-prostaglandin J_2 nanocapsules.

and OPG in the new bone area was detected between the S and K groups [Table 4].

Discussion

The most difficult goals in effectively treating periodontal disease might be the inhibition of the inflammatory condition and the repair of lost alveolar bone. In the present study, we explored the anti-inflammatory and osteogenetic activities of 15d-PGJ_2-NC in a rat model of an artificially created critical bone defect. Our findings provided a scientific basis for the potential application of 15d-PGJ_2-NC in the treatment of periodontitis.

Many studies have reported the anti-inflammatory properties of 15d-PGJ_2,[11,12,29] which might be more effective in regulating inflammatory conditions when loaded in PLGA nanocapsules. In the current study,

Table 4: Semi-quantitative evaluation of expression of EphrinB2 and OPG in the cortical defects after immunohistochemical staining

Groups ($n = 3$)	EphrinB2				OPG			
	Day 3	Day 7	Day 14	Day 28	Day 3	Day 7	Day 14	Day 28
S	7.47 ± 0.46	9.24 ± 0.22	11.99 ± 0.54	9.58 ± 0.31	6.37 ± 0.29	5.37 ± 0.17	3.41 ± 0.45	1.50 ± 0.12
K	8.66 ± 0.10	11.71 ± 0.06	10.03 ± 0.67	5.75 ± 0.29	5.46 ± 0.51	5.60 ± 0.33	4.48 ± 0.30	2.53 ± 0.19
F	12.42 ± 0.80*	14.11 ± 0.66*	13.92 ± 0.79	11.65 ± 0.67†	7.52 ± 0.33	8.95 ± 0.06	8.12 ± 0.11*	3.73 ± 0.33†
N	18.14 ± 0.45*,†	21.57 ± 0.54*,†,‡	19.05 ± 0.70*,†	16.7 ± 0.74*,†	9.56 ± 0.44*,†	13.67 ± 0.42*,†,‡	11.28 ± 0.33*,†,‡	5.61 ± 0.48*,†

Three sections from each defect were obtained on days 3, 7, 14, and 28. The positive area of immunostaining was calculated automatically and presented as a percentage of the total cortical defect area. Values represent the mean ± SD of three sections. *P<0.05 versus groups S; †P<0.05 versus groups K; ‡P<0.05 versus groups F. OPG: Osteoprotegerin; S: Saline; K: Empty nanocapsules; F: Free 15-Deoxy-$\Delta^{12,14}$-prostaglandin J_2; N: 15-Deoxy-$\Delta^{12,14}$-prostaglandin J_2 nanocapsules; SD: Standard deviation.

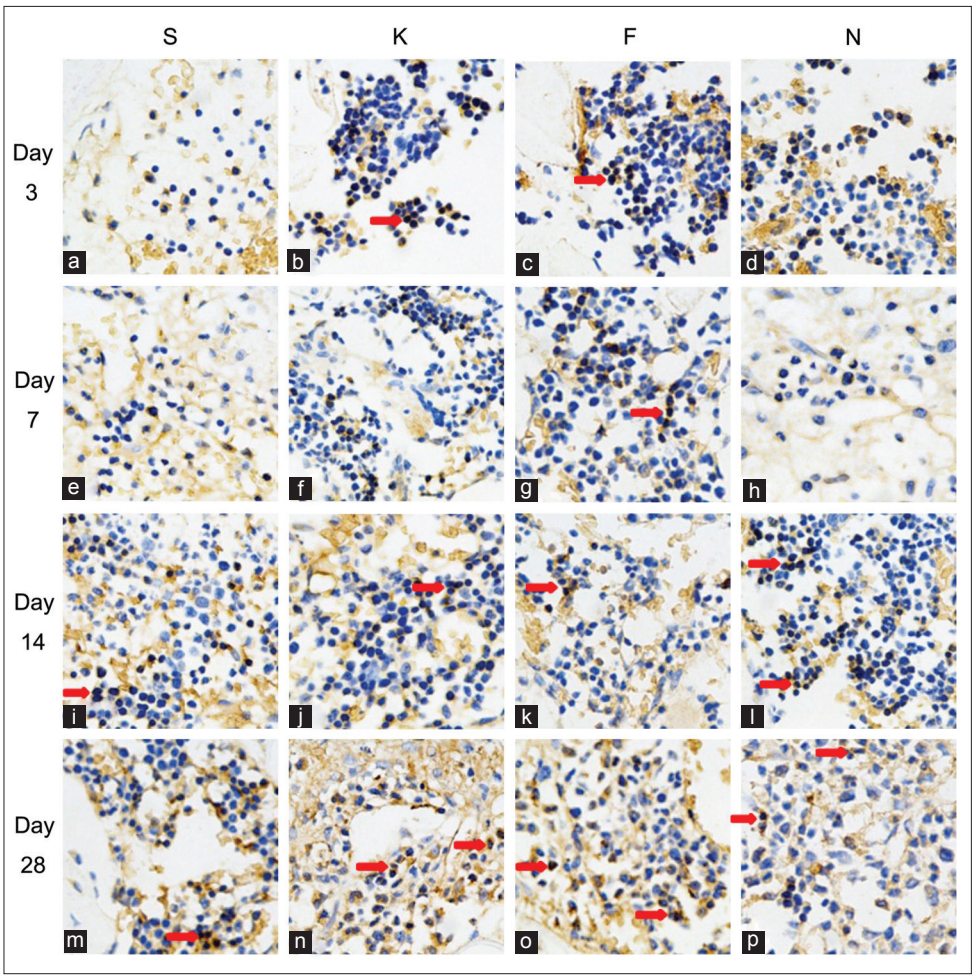

Figure 3: Effect of 15d-PGJ_2 on EphrinB2 expression in the cortical defect area. Specimens were obtained from animals treated with saline (a, e, i and m), empty nanocapsules (b, f, j and n), free 15d-PGJ_2 (c, g, k and o), and 15d-PGJ_2-NC (d, h, l and p) on days 3 (a-d), 7 (e-h), 14 (i-l), and 28 (m-p) after surgery. Red arrows indicated the positive staining cells (Immunohistochemical, original magnification ×400). 15d-PGJ_2-NC: 15-Deoxy-$\Delta^{12,14}$-prostaglandin J_2 nanocapsules.

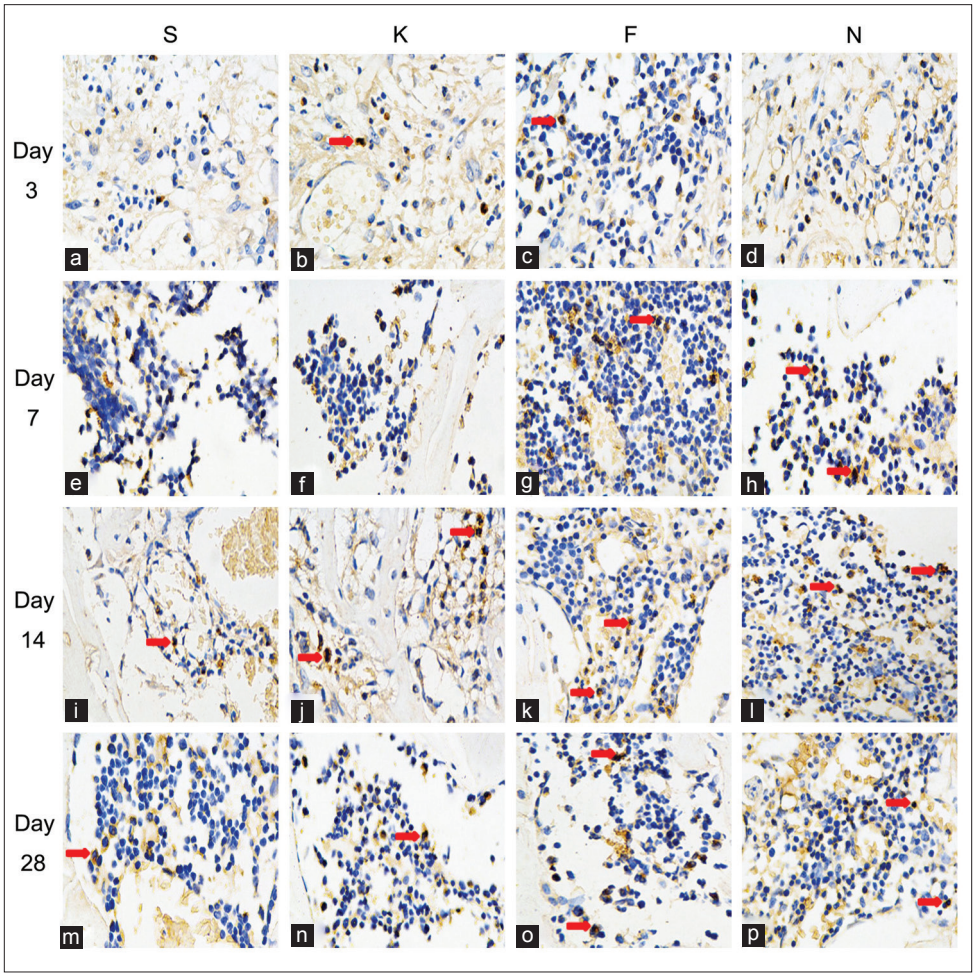

Figure 4: Effect of 15d-PGJ_2 on OPG expression in the cortical defect area. Specimens were obtained from animals treated with saline (a, e, i, and m), empty nanocapsules (b, f, j and n), free 15d-PGJ_2 (c, g, k and o), and 15d-PGJ_2-NC (d, h, l and p) on days 3 (a-d), 7 (e-h), 14 (i-l), and 28 (m-p) after surgery. Red arrows indicated the positive staining cells (Immunohistochemical, original magnification ×400). 15d-PGJ_2-NC: 15-Deoxy-$\Delta^{12,14}$-prostaglandin J_2 nanocapsules; OPG: Osteoprotegerin.

PLGA nanocapsules with 15d-PGJ_2 were prepared with suitable characteristics, as described above. Although both 15d-PGJ_2-NC and 15d-PGJ_2 could decrease the levels of IL-6, IL-1β, and TNF-α in the defect area and surrounding soft tissue based on Western blot and RT-PCR analysis on days 1, 3, 7, and 14, effects of 15d-PGJ_2-NC were more evident with statistically significant differences when compared with controls. The results indicated that the anti-inflammatory activity of 15d-PGJ_2 was improved by the formulation, which might allow for its gradual release from PLGA nanocapsules.

According to previous data, low doses of 15d-PGJ_2 were found to induce osteoblast activity *in vitro*.[13] In the current study, we demonstrated that the new bone volume in the cortical defect area *in vivo* was increased by both 15d-PGJ_2 and 15d-PGJ_2-NC, but the effect of the latter reached statistical significance on days 14 and 28. On day 7, we also found more immature bone trabeculae near the medulla in the 15d-PGJ_2-NC-treated animals compared with other groups. To investigate the potential mechanism of 15d-PGJ_2-induced new bone formation, qRT-PCR and immunohistochemical staining were used to detect the levels of several factors known to modulate bone formation, including BMP-6, PDGF-B, EphrinB2, and OPG. As determined by qRT-PCR, PDGF-B was statistically significantly upregulated by 15d-PGJ_2-NC, compared with the control group, and this difference was most obvious on day 1 after the surgery. In addition, 15d-PGJ_2-NC also enhanced BMP-6 gene expression, compared with that in control animals. The mRNA expression levels of BMP-6 and PDGF-B were also only slightly increased in 15d-PGJ_2-treated animals. The empty nanocapsules had neither a positive nor negative effect on the expression of BMP-6 and PDGF-B. These data indicated the possible osteogenetic effect of 15d-PGJ_2-NC during the healing process of bone.

As revealed by immunohistochemical staining, EphrinB2 showed stronger and more intense signals in 15-Deoxy-$\Delta^{12,14}$-PGJ_2-NC-treated animals, correlating with the observed increase in new bone formation, compared with other groups. In the control animals, the protein expression of EphrinB2 started to increase from day 3,

peaked on day 14, and then declined on day 28. In contrast, EphrinB2 protein levels peaked on day 7 and declined by the end of the study in 15d-PGJ_2-NC-treated animals. 15d-PGJ_2 also increased the level of EphrinB2, but only with a statistically significant difference on days 3 and 7. Immunostaining of OPG demonstrated a relatively weak expression in both osteocytes and bone lining cells. The area of positive staining for OPG was largest on day 3 and decreased in a time-dependent fashion on days 7, 14, and 28 in control animals. Meanwhile, interference by 15d-PGJ_2-NC resulted in the appearance of the greatest OPG-positive staining area on day 7. These immunostaining results suggested that 15d-PGJ_2-NC might have increased the levels and prolonged the duration of EphrinB2 and OPG protein expression. While BMP-6 and PDGF-B were known to be involved in modulating recruitment, proliferation, and differentiation of osteoprogenitor cells, EphrinB2 and OPG played important roles in promoting the differentiation and maturation of osteoblasts and inhibiting the differentiation of osteoclasts.[26,27] As the receptor of EphrinB2, EphB4, and EphrinB2 composed the pathway adjusting the osteoblast and osteoclast differentiation for the bone homeostasis, it was found that EphB4's and EphrinB2's expression in osteoblast surface could activate each other.[26] Typically, the stimulation of EphB4 by EphrinB2 produced a positive signal to promote osteoblast differentiation and maturation. Conversely, the inversion signal of EphB4 activation of EphrinB2, inhibited the differentiation of osteoclasts. In the present study, the increased new bone formation by 15d-PGJ_2-NC might be related to the regulation of differentiation of both osteoblasts and osteoclasts induced by the elevated expression of these bone-related factors.

In the current study, the observed decrease in pro-inflammatory cytokines and increase in the expression of growth factors were accompanied by an increase in new bone volume. However, more studies are needed to clarify whether the increase of new bone formation induced by 15d-PGJ_2 was attributed to the reduction of inflammatory response mediated by IL-6, IL-1β, and TNF-α or the activation of bone cells. Due to the limitation of the present study, 99.8% 15d-PGJ_2 has been released from the PLGA nanoparticles within 360 min. Further studies on other methods such as 3-dimensional printing nano-scaffold for improved control release of 15d-PGJ_2 should be investigated.

In conclusion, the delivery of 15d-PGJ_2 not only clearly decreased inflammatory mediators, shifting the inflammatory response to a rapid resolution of inflammation, but also showed the potential to promote the process of bone repair by increasing the relevant bone growth factors. These findings altogether indicated that the 15d-PGJ_2 might be a potentially useful therapeutic agent for a wide range of complex inflammatory conditions involving bone disorders, including periodontal diseases.

Supplementary information is linked to the online version of the paper on the Chinese Medical Journal website.

Financial support and sponsorship

This work was supported by grants from the National Natural Science Foundation of China (No. 81300881, No. 20141402, No. 81271142, and No. 81400510), the Science and Technology Department of Zhejiang Province (No. 2012C33009), and the Doctoral Program of Higher Education of China (No. 20130101110011).

Conflicts of interest

There are no conflicts of interest.

References

1. Kajiya M, Giro G, Taubman MA, Han X, Mayer MP, Kawai T. Role of periodontal pathogenic bacteria in RANKL-mediated bone destruction in periodontal disease. J Oral Microbiol 2010;2. doi: 10.3402/jom.v2i0.5532.
2. Haffajee AD, Socransky SS. Microbial etiological agents of destructive periodontal diseases. Periodontol 2000 1994;5:78-111. doi: 10.1111/j.1600-0757.1994.tb00020.x.
3. Bascones A, Noronha S, Gómez M, Mota P, Gónzalez Moles MA, Villarroel Dorrego M. Tissue destruction in periodontitis: Bacteria or cytokines fault? Quintessence Int 2005;36:299-306. doi: 10.1016/j.tripleo.2004.07.021
4. Okada H, Murakami S. Cytokine expression in periodontal health and disease. Crit Rev Oral Biol Med 1998;9:248-66. doi: 10.1177/10454411980090030101.
5. Hasturk H, Kantarci A, Goguet-Surmenian E, Blackwood A, Andry C, Serhan CN, *et al.* Resolvin E1 regulates inflammation at the cellular and tissue level and restores tissue homeostasis *in vivo*. J Immunol 2007;179:7021-9. doi: 10.4049/jimmunol.179.10.7021.
6. Repeke CE, Ferreira SB Jr., Vieira AE, Silveira EM, Avila-Campos MJ, da Silva JS, *et al.* Dose-response met-RANTES treatment of experimental periodontitis: A narrow edge between the disease severity attenuation and infection control. PLoS One 2011;6:e22526. doi: 10.1371/journal.pone.0022526.
7. Surh YJ, Na HK, Park JM, Lee HN, Kim W, Yoon IS, *et al*. 15-Deoxy-Δ 12,14-prostaglandin J2, an electrophilic lipid mediator of anti-inflammatory and pro-resolving signaling. Biochem Pharmacol 2011;82:1335-51. doi: 10.1016/j.bcp.2011.07.100.
8. Scher JU, Pillinger MH. 15d-PGJ2: The anti-inflammatory prostaglandin? Clin Immunol 2005;114:100-9. doi: 10.1016/j.clim.2004.09.008.
9. Gilroy DW, Colville-Nash PR, McMaster S, Sawatzky DA, Willoughby DA, Lawrence T. Inducible cyclooxygenase-derived 15-deoxy (Delta) 12-14PGJ2 brings about acute inflammatory resolution in rat pleurisy by inducing neutrophil and macrophage apoptosis. FASEB J 2003;17:2269-71. doi: 10.1096/fj.02-1162fje.
10. Gilroy DW, Lawrence T, Perretti M, Rossi AG. Inflammatory resolution: New opportunities for drug discovery. Nat Rev Drug Discov 2004;3:401-16. doi: 10.1038/nrd1383.
11. Jung WK, Park IS, Park SJ, Yea SS, Choi YH, Oh S, *et al.* The 15-deoxy-Delta12,14-prostaglandin J2 inhibits LPS-stimulated AKT and NF-kappaB activation and suppresses interleukin-6 in osteoblast-like cells MC3T3E-1. Life Sci 2009;85:46-53. doi: 10.1016/j.lfs.2009.04.010.
12. Napimoga MH, da Silva CA, Carregaro V, Farnesi-de-Assunção TS, Duarte PM, de Melo NF, *et al.* Exogenous administration of 15d-PGJ2-loaded nanocapsules inhibits bone resorption in a mouse periodontitis model. J Immunol 2012;189:1043-52. doi: 10.4049/jimmunol.1200730.
13. Napimoga MH, Demasi AP, Bossonaro JP, de Araújo VC, Clemente-Napimoga JT, Martinez EF. Low doses of 15d-PGJ2 induce osteoblast activity in a PPAR-gamma independent manner. Int Immunopharmacol 2013;16:131-8. doi: 10.1016/j.intimp.2013.03.035.
14. Clemente-Napimoga JT, Moreira JA, Grillo R, de Melo NF, Fraceto LF, Napimoga MH. 15d-PGJ2-loaded in nanocapsules

enhance the antinociceptive properties into rat temporomandibular hypernociception. Life Sci 2012;90:944-9. doi: 10.1016/j.lfs.2012.04.035.
15. Alves C, de Melo N, Fraceto L, de Araújo D, Napimoga M. Effects of 15d-PGJ2-loaded poly(D,L-lactide-co-glycolide) nanocapsules on inflammation. Br J Pharmacol 2011;162:623-32. doi: 10.1111/j.1476-5381.2010.01057.x.
16. Kishimoto T. Interleukin-6: Discovery of a pleiotropic cytokine. Arthritis Res Ther 2006;8 Suppl 2:S2. doi: 10.1186/ar1916.
17. Gabay C. Interleukin-6 and chronic inflammation. Arthritis Res Ther 2006;8 Suppl 2:S3. doi: 10.1186/ar1917.
18. Nagy Z, Radeff J, Stern PH. Stimulation of interleukin-6 promoter by parathyroid hormone, tumor necrosis factor alpha, and interleukin-1beta in UMR-106 osteoblastic cells is inhibited by protein kinase C antagonists. J Bone Miner Res 2001;16:1220-7. doi: 10.1359/jbmr.2001.16.7.1220.
19. Hogan BL. Bone morphogenetic proteins: Multifunctional regulators of vertebrate development. Genes Dev 1996;10:1580-94. doi: 10.1101/gad.10.13.1580.
20. Damrongsri D, Geva S, Salvi GE, Cooper LF, Limwongse V, Offenbacher S. Effects of Delta12-prostaglandin J2 on bone regeneration and growth factor expression in rats. Clin Oral Implants Res 2006;17:48-57. doi: 10.1111/j.1600-0501.2005.01181.x.
21. Gitelman SE, Kirk M, Ye JQ, Filvaroff EH, Kahn AJ, Derynck R. Vgr-1/BMP-6 induces osteoblastic differentiation of pluripotential mesenchymal cells. Cell Growth Differ 1995;6:827-36. doi: 10.1016/0143-4160(95)90049-7.
22. Damrongsri D, Geva S, Salvi GE, Williams RC, Limwongse V, Offenbacher S. Cyclooxygenase-2 inhibition selectively attenuates bone morphogenetic protein-6 synthesis and bone formation during guided tissue regeneration in a rat model. Clin Oral Implants Res 2006;17:38-47. doi: 10.1111/j.1600-0501.2005.01187.x.
23. Sun H, Yang HL. Calcium phosphate scaffolds combined with bone morphogenetic proteins or mesenchymal stem cells in bone tissue engineering. Chin Med J 2015;128:1121-7. doi: 10.4103/0366-6999.155121.
24. Chiu HC, Chiang CY, Tu HP, Wikesjö UM, Susin C, Fu E. Effects of bone morphogenetic protein-6 on periodontal wound healing/regeneration in supraalveolar periodontal defects in dogs. J Clin Periodontol 2013;40:624-30. doi: 10.1111/jcpe.12075.
25. Zhang Y, Cheng N, Miron R, Shi B, Cheng X. Delivery of PDGF-B and BMP-7 by mesoporous bioglass/silk fibrin scaffolds for the repair of osteoporotic defects. Biomaterials 2012;33:6698-708. doi: 10.1016/j.biomaterials.2012.06.021.
26. Zhao C, Irie N, Takada Y, Shimoda K, Miyamoto T, Nishiwaki T, *et al.* Bidirectional ephrinB2-EphB4 signaling controls bone homeostasis. Cell Metab 2006;4:111-21. doi: 10.1016/j.cmet.2006.05.012.
27. Walsh MC, Choi Y. Biology of the RANKL-RANK-OPG system in immunity, bone, and beyond. Front Immunol 2014;5:511. doi: 10.3389/fimmu.2014.00511.
28. Ugay L, Kochetkova E, Nevzorova V, Maistrovskaia Y. Role of osteoprotegerin and receptor activator of nuclear factor-κB ligand in bone loss related to advanced chronic obstructive pulmonary disease. Chin Med J 2016;129:1696-703. doi: 10.4103/0366-6999.185857.
29. Liu D, Geng Z, Zhu W, Wang H, Chen Y, Liang J 15-deoxy-Δ 12,14-prostaglandin J2 ameliorates endotoxin-induced acute lung injury in rats. Chin Med J 2014;127:815-20. doi: 10.3760/cma.j.issn.0366-6999.